NANO LETTERS

Letter

pubs.acs.org/NanoLett

Room Temperature Electrical Manipulation of Giant Magnetoresistance in Spin Valves Exchange-Biased with $BiFeO_3$

Julie Allibe,[†] Stéphane Fusil,[†,‡] Karim Bouzehouane,[†] Christophe Daumont,[†] Daniel Sando,[†] Eric Jacquet,[†] Cyrille Deranlot,[†] Manuel Bibes,[†] and Agnès Barthélémy*[,†]

[†]Unité Mixte de Physique CNRS/Thales, 1 Av. A. Fresnel, Campus de l'Ecole Polytechnique, 91767 Palaiseau, France, and Université Paris-Sud, 91405 Orsay, France

[‡]Université d'Evry-Val d'Essonne, Bd. F. Mitterrand, 91025 Evry cedex, France

ABSTRACT: Magnetoelectric multiferroics are attractive materials for the development of low-power electrically controlled spintronic devices. Here we report the optimization of the exchange bias as well as the giant magnetoresistance effect (GMR) of spin valves deposited on top of $BiFeO_3$-based heterostructures. We show that the exchange bias can be electrically controlled through a change in the relative proportion of 109° domain walls and propose solutions toward a reversible process.

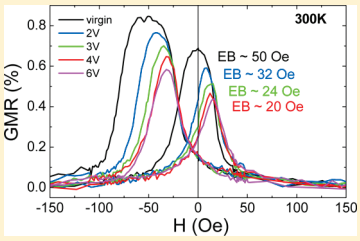

KEYWORDS: *Spintronics, multiferroic, magnetoelectric, nanodomains, $BiFeO_3$, spin valve*

The recent interest in multiferroics,[1,2] materials in which at least two ferroic or antiferroic orders coexist, is motivated by fundamental aspects as well as by their possible applications, particularly in the field of spintronics.[3] Multiferroic compounds are scarce in nature, and the very few that are simultaneously ferromagnetic and ferroelectric usually order well below room temperature, impeding their use in practical applications. Ferroelectric antiferromagnets (FE-AFM) are more common, and some exhibit a coupling between their two order parameters. This magnetoelectric (ME) coupling allows the reversal of the ferroelectric (FE) polarization by a magnetic field[4] or the control of the magnetic order by an electric field.[5] When combined with standard ferromagnets (FM), their AFM character can be used to induce exchange bias. The magnetoelectric coupling allows control of the exchange bias via an electric field, enabling manipulation of the FM layer by purely electrical means. This capability should lead to electrically writable spintronics devices.[6−9] This approach was proven to be effective recently with the demonstration of such control in heterostructures combining the multiferroics $YMnO_3$[10] or $LuMnO_3$[11] and the FM NiFe. However, these reports were of systems that are limited to low-temperature operation. The room temperature control of exchange bias could be realized with $BiFeO_3$ (BFO), the only multiferroic with ordering temperatures well above 300K. This material is a rhombohedral G-type AFM with a Néel temperature T_N of about 640 K,[12] a robust FE with a high Curie temperature T_C of about 1100 K,[13] and a very large polarization of 100 $\mu C/cm^2$ pointing along the [111] direction of the pseudocubic structure.[14] Reports indicate that only a small biquadratic ME coupling between the two order parameters exists in the bulk due to the occurrence of an additional cycloidal modulation of the magnetic order.[15]

Comparably large polarization values have been reported in thin films[16] in which the absence of cycloidal modulation allows for the existence of a linear ME coupling.[17] The coupling between the two orders has been evidenced at the nanoscale through the observation of coupled FE and AFM domains[18] enabling electrical control of the BFO AFM state.[5] Additionally, a large exchange bias, attributed to pinned uncompensated spins,[19] has been demonstrated using BFO thin films capped with transition metal ferromagnets.[20−22] Furthermore, the manipulation of the magnetic state of CoFe dots on top of a BFO layer was recently reported using synchrotron-based techniques and a planar geometry to switch the ferroelectric.[23] From a device point of view, it is essential to work in the vertical geometry that allows operation at moderate voltages, being thereby compatible with standard integrated electronics. This requires the problem of high leakage current in this material[24] be addressed. In order to optimize both the exchange bias and leakage-free FE properties, we recently proposed[25] a bilayer strategy combining BFO and BFO doped with Mn (BFO-Mn), known to drastically reduced the leakage.[26] We found a large exchange bias field of around 50 Oe and a dramatic reduction of the leakage were reported in CoFeB (4 nm)/BFO (10 nm)/BFO-Mn (60 nm)/$SrRuO_3$ (25 nm)//$SrTiO_3$(001).[25] Here we report our efforts in optimizing the exchange bias as well as the giant magnetoresistance effect (GMR) of a spin valve deposited on top of BFO (10 nm)/BFO-Mn (60 or 140 nm)/$SrRuO_3$ (25 nm)//$SrTiO_3$(001). We demonstrate control of the exchange bias by purely electrical means, explain its irreversibility, and propose potential alternatives for reversible device operation.

Received: July 25, 2011
Revised: January 19, 2012
Published: January 23, 2012

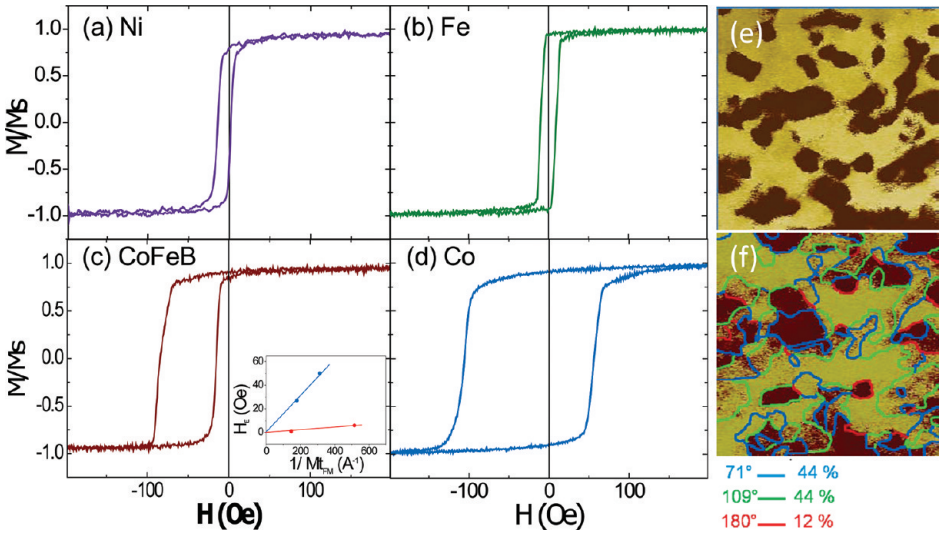

Figure 1. (a–d) Exchange bias for different 4 nm FM/BFO/BFO-Mn samples. Typical out-of-plane (e) and in-plane (f) PFM images of ferroelectric domain pattern and DW analysis of the BFO-Mn/BFO bilayer. The scan area is 1 × 1 μm^2. Inset: corresponding evolution of the exchange bias as a function of $1/Mt_{FM}$.

BFO(10 nm)/BFO-Mn(60 or 140 nm) bilayers (BFO/BFO-Mn) were grown by pulsed laser deposition on 25 nm $SrRuO_3$ (SRO)-coated (001)-$SrTiO_3$ (STO) substrates using a frequency-tripled λ = 355 nm Nd:yttrium aluminum garnet laser at a frequency of 2.5 Hz. The conductive metallic oxide SRO bottom electrode was grown at a deposition temperature T_{dep} = 700 °C in an oxygen pressure P_{dep} = 0.1 mbar. The BFO and BFO-Mn layers were deposited at 580 °C in an oxygen pressure of 6 × 10^{-3} mbar.[27,28] After deposition, the oxide heterostructures were cooled down to room temperature in an oxygen pressure of 300 mbar. The FM layers and the spin valves (trilayer structure FM/M/FM) were sputtered on the BFO/BFO-Mn bilayers at room temperature and protected from oxidation by a 6 nm Au capping layer. A magnetic field of about H_{growth} = 200 Oe was applied during the growth of the first FM to establish an exchange bias interaction with the underlying BFO.

Figure 1 shows magnetization vs magnetic field hysteresis cycles for different 4 nm thick FM films grown on top of BFO (Ni, Fe, $Co_{72}Fe_8B_{20}$ (CoFeB), and Co; all of these FM were deposited on different pieces of the same BFO(10 nm)/BFO-Mn(60 nm) sample). Large shifts in the hysteresis loops as well as enlarged coercive fields are observed depending on the considered FM. The shifts in the loops are generally attributed to the coupling between the spins of the FM and pinned uncompensated spins in the AFM, whereas the increase of the coercive field is related to coupling between unpinned uncompensated spins of the AFM and the spins of the FM. At first glance, it turns out that the coupling between the spins of the FM and the uncompensated spins of the AFM is much less efficient for Ni and Fe than for Co and CoFeB. The corresponding exchange bias and coercive fields are summarized in Table 1. Within the model of exchange bias by Meikeljohn and Bean,[30] one expects H_E to vary as $H_E = -J_{eb}/(\mu_0 M t_{FM})$. As shown in the inset of Figure 1c, two different linear variations are obtained for Co and CoFeB and for Ni and Fe. In the more recent random field model of EB proposed by Malozemoff,[29] the interfacial coupling constant J_{eb} is related to the exchange coupling parameter between the FM and the AFM (J_{ex}), to the spin in the FM and AFM (S_{FM} and S_{AFM}), to the distance between S_{FM} and S_{AFM} (a), and to the AFM domain size (L) by $J_{eb} = \zeta J_{ex} S_{FM} S_{AFM}/aL$. ζ is a geometrical parameter of the order of unity. Because the AF domain size and the AF domain perimeter are proportional, the exchange field may also be considered as being related to the total length of domain walls (DW). It is possible to deduce ζJ_{ex} considering S_{AFM} = 5/2, S_{FM} = 1/2, a = 3.96 Å, and L = 80 nm (value from ref 25 in good agreement with the domain size extracted from piezoresponse force microscopy (PFM) images of the pristine state shown in Figure 1e) from the slopes of these variations. The coupling between Co or CoFeB and BFO correspond to ζJ_{ex} = 3.9 × 10^{-22} J, a value close to the bulk exchange interaction of BFO found by Ruette et al. (5 × 10^{-22} J).[32] For Ni and Fe, the coupling constant has a much lower value of ζJ_{ex} = 0.28 × 10^{-22} J; i.e., the exchange at the interface is reduced by 93%, excluding these materials from practical applications.

Table 1. Exchange Bias and Coercive Fields of 4 nm FM/BFO/BFO-Mn Samples

	H_E (Oe)	H_C (Oe)	M (emu/cm^3)
Ni	−6	7	485
CoFeB	−50	35	800
Co	−25	75	1400
Fe	−1	10	1700

Interestingly, a later development found that the link between exchange bias and domain wall length is restricted to 109° DWs.[31] Following Martin and co-workers,[31] we analyzed our out-of-plane (Figure 1e) and in-plane PFM contrasts (Figure 1f) in detail to identify the different types of domain walls (71°, 109°, and 180°) and found the relative proportions of 109°, 71°, and 180° DWs close to 44%, 44%, and 12%, respectively.

Next we optimized the giant magnetoresistance (GMR) for the spin valves deposited on BFO, ensuring that strong exchange bias was maintained. Different sets of trilayered spin valves were grown, capped with Au, and patterned into stripes by standard optical lithography. A sketch and a photograph of the final device are shown in Figure 2a,b. The stripes were typically 200 μm long and between 2 and 30 μm wide. The

dx.doi.org/10.1021/nl202537y | Nano Lett. 2012, 12, 1141–1145

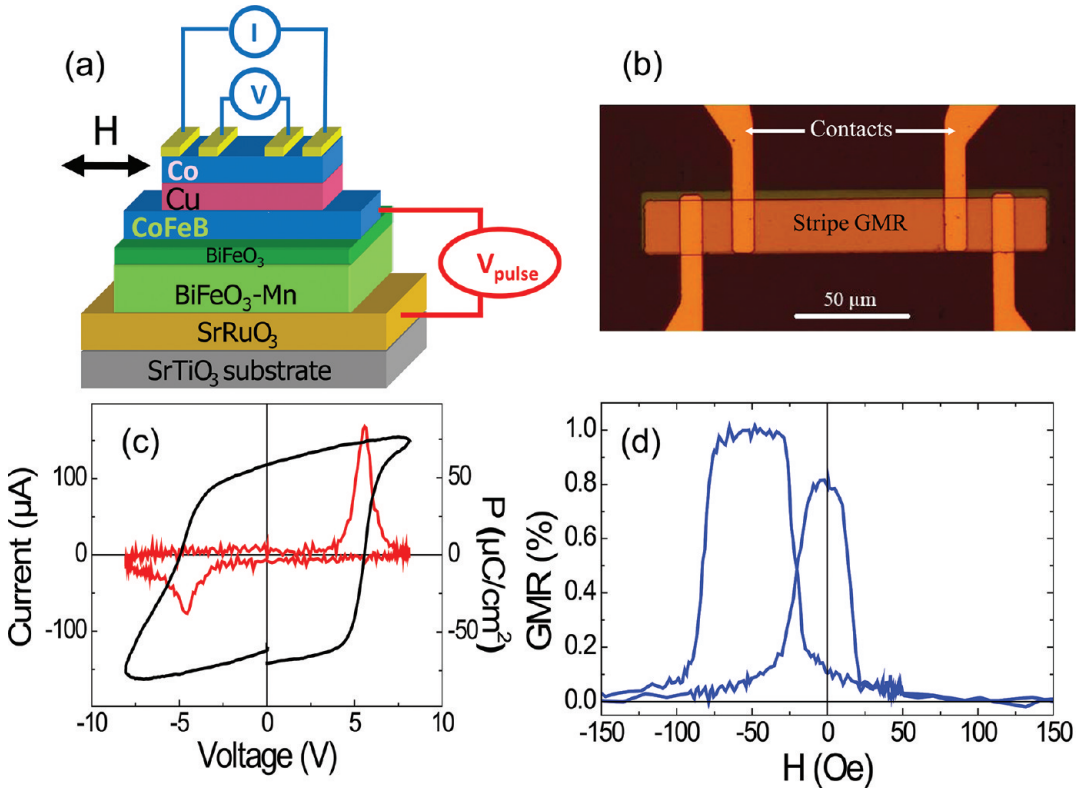

Figure 2. (a) Schematic of the device, (b) micrograph of the stripe with the electrical contacts, and (c) current and polarization versus electric field for a BFO/BFO-Mn bilayer. (d) Giant magnetoresistance of a Au 6 nm/Co 4 nm/Cu 4 nm/CoFeB 4 nm spin valve after patterning (30×185 μm^2 stripe).

distances between the contacts (see Figure 2b) were around 100 and 150 μm for the internal and external contacts, respectively.

The ferroelectric properties of the BFO/BFO-Mn bilayers after patterning were investigated by standard polarization versus electric field $P(E)$ loops with a commercial TF Analyzer 2000 from aixACCT at a frequency of 1 kHz with the bias applied between the $SrRuO_3$ bottom electrode and the GMR spin valve deposited on top. A typical ferroelectric hysteresis loop is presented in Figure 2c. The current vs voltage curve shows clear switching peaks with negligible leakage current. Although the leakage is larger than in previously reported cycles for similar heterostructures with smaller Au top pads,[25] the slight increase observed here may be due to the presence of incomplete d shells in the magnetic electrodes.[33] A remnant polarization of around 60 $\mu C/cm^2$ and coercive voltages in the 4.0−5.5 V range (corresponding to coercive fields of 57−79 MV/m) were observed, which are in good agreement with previously reported values.[25] Figure 2d presents a typical GMR curve of a Au(6 nm)/Co(4 nm)/Cu(4 nm)/CoFeB(4 nm) spin valve after stripe patterning. A standard GMR curve and preserved exchange bias are observed. The resistance switching at $H = -21$ and 17 Oe correspond to the reversal of the Co layer and those at −82 and −23 Oe to the reversal of the CoFeB layer exchange-biased with the BFO/BFO-Mn. From these values an exchange bias field at about −50 Oe is found. The corresponding GMR effect amounts to ∼1%.

To investigate the potential of electrically controlling the magnetic configuration of the spin valve via the FE microstructure,[19] we applied voltage pulses of increasing amplitude between the $SrRuO_3$ and Au electrodes. We varied the pulse duration in the range of 500 μs to several seconds. Figure 3 presents typical GMR curves obtained after different poling

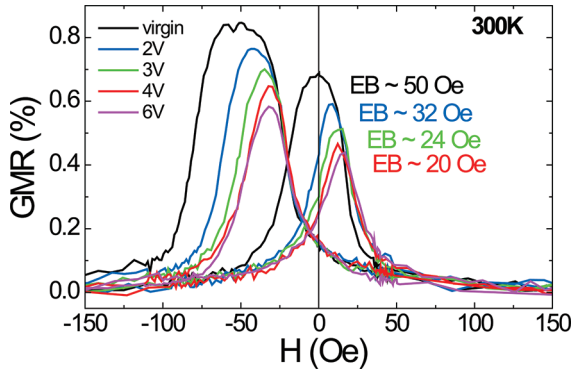

Figure 3. (a) GMR curves of a Au 6 nm/Co 4 nm/Cu 4 nm/CoFeB 4 nm spin valve after different poling events applied to the BFO/BFO-Mn bilayer. The stripe is 210 μm long and 20 μm wide.

events. As the amplitude of the voltage pulse applied to BFO/BFO-Mn increases from 0 to 4 V, the exchange bias (determined from the switching fields of the GMR curves) progressively decreases down to around 20 Oe above 5 V for this heterostructure. This reduction in the exchange bias results in a less well-defined antiparallel state: the GMR curves then become less square, and their amplitude decreases. *This observation clearly demonstrates the manipulation of the resistance of a spin valve by purely electrical means.* However, this process is irreversible, and we did not succeed to restore any exchange

dx.doi.org/10.1021/nl202537y | *Nano Lett.* 2012, 12, 1141−1145

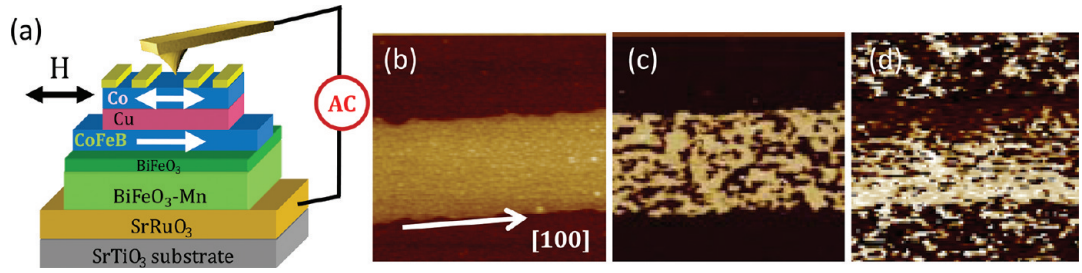

Figure 4. PFM characterization images (6 × 6 μm^2) of the ferroelectric microstructure under a CoFeB pad: (a) sketch of the experiment, (b) topography, (c) out-of-plane PFM phase, and (d) in-plane PFM phase. The reading bias was 1 V.

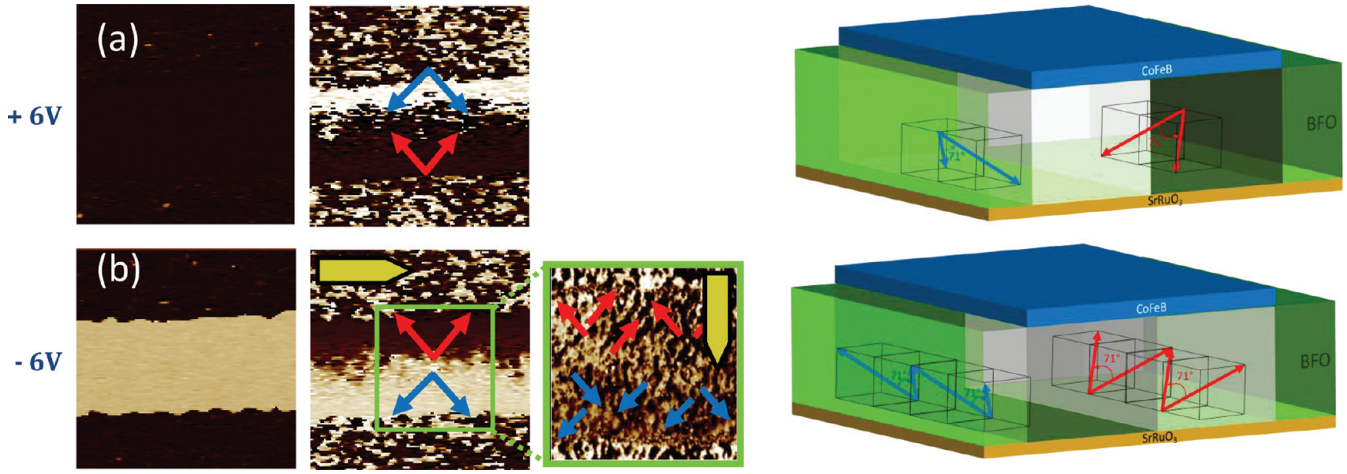

Figure 5. PFM imaging (out-of-plane (left) and in-plane (middle) PFM phase) after poling at +6 V (a) and −6 V (b) and illustration of the observed ferroelectric domains (right). These images were taken in the same location as those of Figure 4, and the reading bias was 1 V. Middle right of (b): in-plane PFM phase after a 90° rotation.

bias by applying voltage with the opposite polarity or by other voltage protocols.

To correlate the irreversible decrease of the exchange bias to the modification of the FE domain configuration at the nanoscale, we performed piezoresponse force microscopy of the BFO/BFO-Mn (PFM, sketch in Figure 4a) through the spin valve (Figure 4b). Both out-of-plane and in-plane components of the ferroelectric polarization can be imaged (Figure 4, c and d, respectively), and the contrast analysis indicates that the eight possible variants of the BFO polarization are indeed present, along with all types of DWs in the pristine state. After poling at $|V_{pulse}| > 6$ V (saturated state, Figure 5a,b), the out-of-plane component of the PFM phase signal becomes homogeneous as expected, but a striking contrast appears in the in-plane component. A possible origin of the unusual bimodal repartition of ferroelectric variants could be a top electrode edge effect which produces lateral electrical stray fields acting on the in-plane component of the polarization. This could explain why this kind of exotic ferroelectric domain structure has not been observed in archetypal FE ($BaTiO_3$ or $PbTiO_3$, for example) with purely out-of-plane polarization. It should be noted that the application of a reading bias of 1 V peak to peak on the pristine state is already enough to initiate modification of the ferroelectric microstructure and generates the early stage of the bimodal structure (Figure 4c) observed more clearly at higher bias (Figure 5).

The domain configuration below the CoFeB stripe electrode is clearly divided into two parts. A complete analysis of the in-plane phase PFM images (of Figure 5a,b) indicates that in each of those areas only 71° DWs are present, irrespective of whether the out-of-plane FE polarization direction is up or down. Rotating the sample by 90° allows the probing of the alternation of the variants along the stripe axis. The in-plane PFM images in this orientation, shown in Figure 5b, indicate that a large number of domains remain after poling and that the average domain size is comparable to that of the pristine state. The ferroelectric microstructures obtained after poling up and down are illustrated in Figure 5a,b. Summarizing this analysis, we conclude that the original proportion of 109° DWs is drastically decreased in the saturated state in which only a small number of 109° DWs may remain in the vicinity of the central stripe long axis. This explains the observed decrease of the exchange bias with electric field, in good agreement with a Malozemoff's model restricted to the 109° DWs.[31] This evolution from the pristine state to a bimodal state where almost only 71° DWs are present is already realized even if a moderate bias, much smaller than the coercive field is applied (see Figure 4d; a reading voltage of 1 V has been used to reveal the ferroelectric domains). Various attempts to restore a significant proportion of 109° DWs were made; for instance by manipulating the polarization with strong ac fields with peak-to-peak amplitude above the coercive value. This "depolarization" did indeed reintroduce some out-of-plane PFM contrast but did not prevent the general trend toward 71° DWs, and furthermore it did not restore any measurable exchange bias.

From these observations and conclusions, similar spin valves deposited on BFO(111) films would provide a more promising system with which to reversibly control a sizable exchange bias by applying pulses. Indeed, in this orientation, the application

dx.doi.org/10.1021/nl202537y | Nano Lett. 2012, 12, 1141−1145

of a vertical electric field may allow the transition from a single domain (with only one variant of the polarization pointing out of the plane) to a polydomain state (with three variants with possible 109° domain wall). Another solution could be to consider a more complex device allowing the application of an in-plane electric field as well as a vertical one.

In summary, we have reported the optimization of the exchange bias as well as the giant magnetoresistance effect (GMR) of a spin valve deposited on top of $BiFeO_3$/Mn doped $BiFeO_3$(001) heterostructures. We demonstrated the modification of this exchange bias and related resistance value of the spin valve by purely electric means. We related this variation to the nanoscale configuration of the AFM-FE domains and domain walls in $BiFeO_3$. Finally, we have proposed possible solutions toward a reversible process.

AUTHOR INFORMATION

Corresponding Author

*E-mail: agnes.barthelemy@thalesgroup.com.

Notes

The authors declare no competing financial interest.

ACKNOWLEDGMENTS

We acknowledge partial financial support by the EU STREP "Macomufi", the ANR P-Nano "Méloïc", the C-Nano Ile-de-France, the PRES Universud, and the Direction Générale de l'Armement.

REFERENCES

(1) Spaldin, N.; M. Fiebig, M. *Science* **2005**, *309*, 391.

(2) Eerenstein, W.; Mathur, N. D.; Scott, J. F. *Nature* **2006**, *442*, 759.

(3) Bibes, M.; Barthélémy, A. *IEEE Trans. Electron Devices* **2007**, *54*, 1003.

(4) Kimura, T.; Goto, T.; Shintani, H.; Ishizaka, K.; Arima, T.; Tokura, Y. *Nature* **2003**, *426*, 55.

(5) Zhao, T.; Scholl, A.; Zavaliche, F.; Lee, K.; Barry, M.; Doran, A.; Cruz, M. P.; Chu, Y. H.; Ederer, C.; Spaldin, N. A.; Das, R. R.; Kim, D. M.; Baek, S. H.; Eom, C. B.; Ramesh, R. *Nature Mater.* **2006**, *5*, 823.

(6) Binek, C.; Hochstrat, A.; Chen, X.; Borisov, P.; Kleemann, W.; Doudin, B. *J. Appl. Phys.* **2005**, *97*, 10C514.

(7) Binek, C.; Doudin, B. *J. Phys.: Condens. Matter.* **2005**, *17*, L39.

(8) Chen, X.; Hochstrat, A.; Borisov, P.; Kleemann, W. *Appl. Phys. Lett.* **2006**, *89*, 202508.

(9) Bibes, M.; Barthélémy, A. *Nature Mater.* **2008**, *7*, 425.

(10) Laukhin, V.; Skumryev, V.; Marti, X.; Hrabovsky, D.; Sanchez, F.; Garcêa-Cuenca, M. V.; Ferrater, C.; Varela, M.; Lüders, U.; Bobo, J. F.; Fontcuberta, J. *Phys. Rev. Lett.* **2006**, *97*, 227201.

(11) Skumryev, V.; Laukhin, V.; Fina, I.; Martí, X.; Sánchez, F.; Gospodinov, M; J. Fontcuberta, J. *Phys. Rev. Lett.* **2011**, *106*, 057206.

(12) Kiselev, S. V.; Ozerov, R. P.; Zhdanov, G. S. *Sov. Phys. Dokl.* **1963**, *7*, 742.

(13) Teague, J. R.; Gerson, R.; James, W. J. *Solid State Commun.* **1970**, *8*, 1073.

(14) Lebeugle, D.; Colson, D.; Forget, A.; Viret, M. *Appl. Phys. Lett.* **2007**, *91*, 022907.

(15) Popov, Yu.F.; Zvezdin, A.; Vorob'ev, G.; Kadomtseva, A.; Murashev, V.; Rakov, D. *JETP Lett.* **1993**, *57*, 69.

(16) Wang, J.; Neaton, J. B.; Zeng, H.; Nagarajan, V.; Ogale, S. B.; Liu, B.; Viehland, D.; Vaithyanathan, V.; Schlom, D. G.; Waghmare, U. V.; Spaldin, N. A.; Rabe, K. M.; Wuttig, M.; Ramesh, R. *Science* **2003**, *299*, 1719.

(17) Béa, H.; Bibes, M.; Petit, S.; Kreisel, J.; Barthelemy, A. *Philos. Mag. Lett.* **2007**, *87*, 165.

(18) Catalan, G.; H. Bea, H.; Fusil, S.; Bibes, M.; Paruch, P.; Barthelemy, A.; Scott, J. F. *Phys. Rev. Lett.* **2008**, *100*, 027602.

(19) Béa, H.; Bibes, M.; Ott, F.; Dupé, B.; Zhu, X.-H.; Petit, S.; Fusil, S.; Deranlot, C.; Bouzehouane, K.; Barthélémy, A. *Phys. Rev. Lett.* **2008**, *100*, 017204.

(20) Béa, H.; Bibes, M.; Cherifi, S.; Nolting, F.; Warot-Fonrose, B.; Petit, S.; Kreisel, J.; Fusil, S.; Herranz, G.; Deranlot, C.; Jacquet, E.; Bouzehouane, K.; Barthélémy, A. *Appl. Phys. Lett.* **2006**, *89*, 242114.

(21) Dho, J.; Qi, X. D; Kim, H.; Macmanus-Driscoll, J. L.; Blamire, M. G. *Adv. Mater.* **2006**, *18*, 1445.

(22) Martin, L. W.; Chu, Y. H.; Zhan, Q.; Ramesh, R. *Appl. Phys. Lett.* **2007**, *91*, 172513.

(23) Chu, Y. H.; Martin, L. W.; Holcomb, M. B.; Gajek, M.; Han, S.-J.; He, Q.; Balke, N.; Yang, C.-H.; Lee, D.; Hu, W.; Zhan, Q.; Yang, P.-L.; Fraile-Rodriguez, A.; Scholl, A.; Wang, S. X.; Ramesh, R. *Nature Mater.* **2008**, *7*, 478.

(24) Pabst, G. W.; Martin, L. W.; Chu, Y. -H.; Ramesh, R. *Appl. Phys. Lett.* **2007**, *90*, 072902.

(25) Allibe, J.; Infante, I. C.; Fusil, S.; Bouzehouane, K.; Jacquet, E.; Deranlot, C.; Bibes, M; Barthélémy, A. *Appl. Phys. Lett.* **2009**, *95*, 182503.

(26) Singh, S. K.; Ishiwara, H.; Maruyama, K. *Appl. Phys. Lett.* **2006**, *88*, 262908.

(27) Béa, H.; Bibes, M.; Barthélémy, A.; Bouzehouane, K.; Jacquet, E.; Khodan, A..; Contour, J.-P.; Fusil, S.; Wyczisk, F.; Forget, A.; Lebeugle, D.; Colson, D.; Viret, M. *Appl. Phys. Lett.* **2005**, *87*, 072508.

(28) Zhu, X. H.; Béa, H.; Bibes, M.; Fusil, S.; Bouzehouane, K.; Jacquet, E.; Barthélémy, A.; Lebeugle, D.; Viret, M.; Colson, D. *Appl. Phys. Lett.* **2008**, *93*, 082902.

(29) Malozemoff, A. P. *Phys. Rev. B* **1987**, *35*, 3679.

(30) Meikeljohn, W. P.; Bean, C. P. *Phys. Rev.* **1956**, *102*, 1413.

(31) Martin, L. W.; Chu, Y. H.; Holcomb, M. B.; Huijben, M.; Yu, P.; Han, S. J.; Lee, D.; Wang, S. X.; Ramesh, R. *Nano Lett.* **2008**, *8*, 2050.

(32) Ruette, B.; Zvyagin, S.; Pyatakov, A. P.; Bush, A.; Li, J. F.; Belotelov, V. I.; Zvezdin, A. K.; Viehland, D. *Phys. Rev. B* **2004**, *69*, 064114.

(33) Pintilie, L.; Vrejoiu, I.; Hesse, D.; Alexe, M. *J. Appl. Phys.* **2008**, *104*, 114101.